Dispersion Behaviors of Molybdena on Titania (Rutile and/or Anatase)

Haiyang Zhu,[†] Mingmin Shen,[†] Yong Wu,[†,‡] Xiaowei Li,[†] Jianming Hong,[§] Bin Liu,[†] Xinglong Wu,[||] Lin Dong,*[,†] and Yi Chen[†]

Key Laboratory of Mesoscopic Chemistry of MOE, College of Chemistry and Chemical Engineering, Center of Modern Analysis, Department of Physics, Nanjing University, Nanjing 210093, China, and Department of Chemistry, Nanjing Normal University, Nanjing 210097, China

Received: February 21, 2005; In Final Form: April 20, 2005

Raman and FT−IR spectra were employed to investigate the dispersion of molybdena on mixed TiO_2 (rutile and anatase, signed as R and A) with different BET surface ratios of rutile/TiO_2(R + A). The results showed that (1) molybdena would preferentially disperse on the rutile surface in mixed TiO_2; (2) for MoO_3/rutile with low molybdena loading (e.g., 0.20 mmol/100 m^2 rutile), a dispersed molybdena species existed on the rutile surface in an isolated tetrahedral coordination environment, while for MoO_3/rutile with high molybdena loading (e.g. 0.82 mmol/100 m^2 rutile), a polymeric molybdena species could be detected on the rutile surface; (3) for the MoO_3/anatase sample, a dispersed molybdena species existed on the anatase surface in a polymeric coordination environment; and (4) the formation of the Bronsted acid site on the surface of rutile and anatase should be related to the polymeric molybdena species. All these results have been discussed via the interaction between OH groups of molybdena and OH groups of rutile and anatase, and it seems reasonable to suggest that, for the lower molybdena loading, the different states of the dispersed molybdena species should result from the different dehydration orders of OH groups of the molybdena and surface OH groups of rutile and anatase.

Introduction

Supported molybdena catalysts have been extensively investigated in the past decades because of their importance in many industrial reactions, such as hydrodesulfurization (HDS), partial oxidation, and metathesis of olefins.[1−7] In many reactions catalyzed by molybdena, however, the active component is often supported on oxide supports including Al_2O_3, TiO_2, SiO_2, and mixed oxides, such as MoO_3/γ-Al_2O_3, MoO_3/SiO_2, MoO_3/TiO_2, MoO_3/ZrO_2, and MoO_3/TiO_2-ZrO_2.[6−9] The efficiency of these catalysts mainly depends on the dispersion of an active phase and the structure of supported molybdena, which would be greatly influenced by the nature of supports and the preparation conditions. Many studies have been carried out to investigate the structure of supported molybdena and the interaction between dispersed molybdena and supports during the last two decades.[8−15]

TiO_2 is widely used in the material, physics, and chemistry fields. As a catalyst support, TiO_2 shows unique properties in various important reactions, such as V_2O_5/TiO_2 in selective oxidation of *o*-xylene to phthalic anhydride, the selective catalytic reduction of NO_x with NH_3, and the oxidation of sulfur dioxide to sulfur trioxide; MoO_3/TiO_2 in the selective photooxidation of alcohol; and $CoO-MoO_3/TiO_2$ in hydrodesulfurization of hydrocarbon oils, etc.[5,16−20] It is well-established that titania exists in three main crystalline forms (i.e., anatase, rutile, and brookite) and that each crystalline structure exhibits different physicochemical properties, which result in the different catalytic properties of supported molybdena on different titania crystalline forms.[15,21,22] Recently, the influence of the two crystallographic modifications of titania (i.e., anatase and rutile) on the active species in those titania-supported catalysts has been the interest of much research. For example, Kim et al. have extensively studied the interaction of molybdena with anatase and rutile. They investigated the physicochemical properties of MoO_3/TiO_2 catalysts and the influence of the structure and corresponding surface properties of adsorbed monolayer species on the catalytic activity of methanol oxidation.[15,21,22] Matsumura et al. reported the synergism between rutile and anatase particles in photocatalytic oxidation of naphthalene.[23]

As known to all, TiO_2, such as P-25 (Degussa, rutile/anatase is about 1:3), is widely used in the catalytic industry.[6,9] However, to our knowledge, little attention has been paid to the possibly individual and/or synergic roles of anatase and rutile in these catalysts. Apparently, it would be quite helpful for understanding the catalytic behaviors of the practical titania (mixture of rutile and anatase) supported metal oxide catalysts to systematically investigate the interaction between supported active species (e.g., molybdena) and the mixture of anatase and rutile with different R/A ratios as well as the physicochemical properties shown in these samples.

IR and Raman spectra are important characterization techniques for supported metal oxide catalysts, especially for MoO_3 and WO_3, which can provide the fundamental molecular level information about the surface properties of supported metal oxide catalysts: molecular structure of the surface metal oxide species, location of the surface metal oxide species, surface coverage of the metal oxide overlayer, and distribution of surface Lewis and Bronsted acid sites by the appropriate probe molecules, etc. In the present work, TiO_2 support was obtained by mechanically mixing anatase and rutile according to the

* To whom correspondence should be addressed. Phone: 86 25 83594945; fax: 86 258 331 7761; e-mail: donglin@nju.edu.cn.
[†] College of Chemistry and Chemical Engineering, Nanjing University.
[‡] Nanjing Normal University.
[§] Center of Modern Analysis, Nanjing University.
[||] Department of Physics, Nanjing University.

10.1021/jp050890a CCC: $30.25
Published on Web 05/21/2005

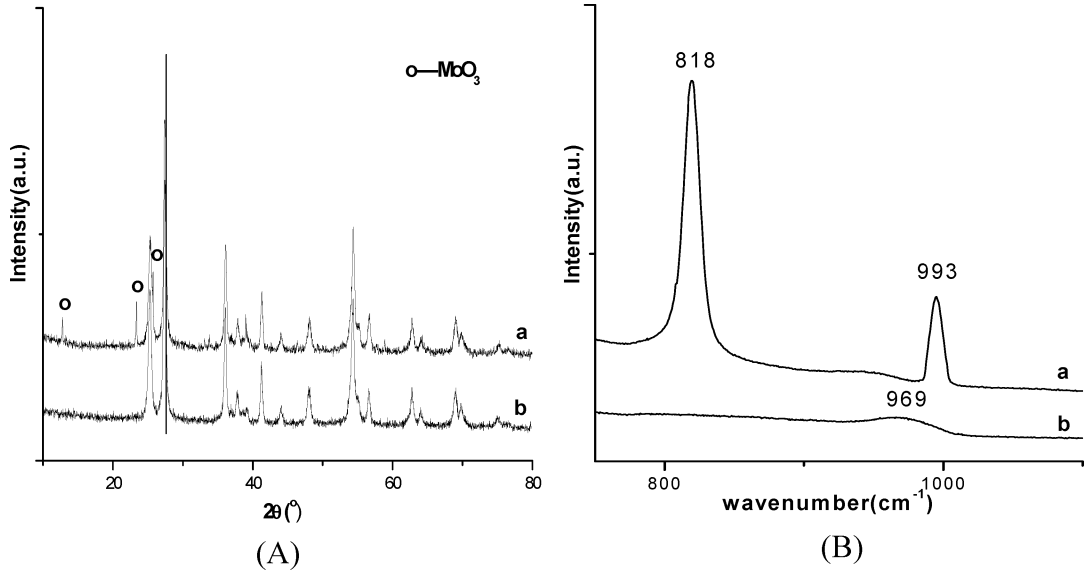

Figure 1. XRD patterns (A) and Raman spectra (B) of 06MoTi-50%r samples before (a) and after calcination (b).

different BET surface area ratio of anatase and rutile. In situ IR and Raman spectra were used to characterize these mixed titania supported molybdena catalysts, and X-ray diffraction (XRD) and temperature-programmed reduction (TPR) were also used as a complementary characterization. Attention is mainly focused on (1) the influence of the different rutile/anatase surface area ratio in mixed TiO_2 on the dispersion behaviors of molybdena and (2) the relationship between the distribution of surface acid sites (Bronsted and Lewis acidities) and the states of the dispersed surface molybdena. A tentative model for the formation and the coordination environment of surface molybdena species in MoO_3/TiO_2 (anatase and/or rutile) has been proposed.

Experimental Procedures

Instrumentation. X-ray diffraction (XRD) qualitative and quantitative analyses were carried out on a Philips X'pert Pro diffractometer using Ni-filtered CuKα radiation (0.15418 nm). The X-ray tube was operated at 40 kV and 40 mA.

Laser Raman spectra (LRS) were recorded using a T64000 spectrometer, Atago-Jobin Yvon, France−Japan, and an Ar^+ laser with an excitation wavelength of 514.5 nm in a macro-mode. A laser power of 300 mW at the sample was applied. No sample preparation is required; three accumulations of 20 s were used in each sample.

In situ Fourier transform infrared spectroscopy (FT−IR) of adsorbed pyridine (Py) was carried out on a Nicolet AVATAR 360 FT−IR instrument running at 4 cm^{-1} resolutions. The nature of the acid sites was investigated using pyridine as the probe molecule. Thin, but intact, self-supporting wafers (≈15 mg) of the adsorbents were prepared and mounted inside a specially designed, heatable and evacuable, all-quartz IR cell. The cell, equipped with CaF_2 windows, was hooked to an all-Pyrex glass Gas/Vac handling system and evacuated to 10^{-4} Torr at 400 °C for 2 h. Then, the wafer was cooled to 27 °C. The cell and wafer background (Bkg) spectra were taken (the average of an accumulated 40 scans) over the frequency range of 4000−400 cm^{-1}. Then, the cell was rehooked to the Gas/Vac line, and Py vapor was expanded into it at 27 °C. After 30 min contact with the sample, physically absorbed bases were evacuated at 150 °C for 2 h. A spectrum of the wafer plus irreversibly adsorbed Py (plus cell Bkg) was taken. By absorption subtraction of the cell and wafer Bkg spectra, IR difference spectra of the gas phase and Py adsorbed species were obtained, respectively.

Temperature-programmed reduction (TPR) was carried out in a quartz U-tube reactor, and a 100 mg sample was used for each measurement. Prior to the reduction, the sample was pretreated in an N_2 stream at 100 °C for 1 h and then cooled to room temperature. After that, a H_2−Ar mixture (7% H_2 by volume) was switched on, and the temperature was increased linearly at a rate of 10 °C min^{-1}. A thermal conductivity cell detected the consumption of H_2 in the reactant stream.

Materials. Anatase support was prepared via hydrolysis of titanium alkoxides. The product was washed, dried, and then calcined in flowing air at 500 °C for 5 h. The BET surface areas of anatase and rutile (JRC-TiO-3, rutile phase) are 77 and 42 m^2/g, respectively. Mixed titania support was prepared by fully grinding the mixture of anatase and rutile, in which the surface area ratio of rutile/TiO_2(R + A) was 0, 25, 50, 75, and 100%. MoO_3/TiO_2(R + A) samples were prepared by heating the mechanical mixture of the required amounts of MoO_3 and TiO_2(R + A) at 450 ×bcC in flowing oxygen for 24 h. For simplicity, MoO_3/TiO_2 samples were noted as xMoTi-y%r, for example, 02MoTi-25%r corresponds to the MoO_3/TiO_2 sample prepared by mechanical mixture with the molybdena loading amount of 0.20 mmol/100 m^2 TiO_2 and when the BET surface area ratio of rutile/TiO_2(R + A) is equal to 25%.

Results and Discussion

Figure 1A,B shows the XRD patterns and Raman spectra of 06MoTi-50%r samples before and after calcination. For the sample before calcination, the peaks centered at $2\theta = 12.8$, 23.4, and 25.8 can be detected in the XRD pattern of Figure 1A, spectrum a, which is attributed to the characteristic diffraction peaks of crystalline MoO_3. The Raman bands corresponding to the stretching vibrations of Mo−O−Mo and Mo═O in crystalline MoO_3 can also be found at 818 and 993 cm^{-1} in the profile of Figure 1B, spectrum a, respectively.[22] After calcination, the diffraction peaks and the Raman bands attributed to crystalline MoO_3 disappear. In addition, a new broad Raman band at about 969 cm^{-1} could be found in the profile of Figure 1B, spectrum b, which should be the Raman signal of a surface molybdena species (i.e., the terminal Mo═O stretching mode of the surface molybdena species).[22] These results suggest that MoO_3 has been dispersed on the surface of mixed TiO_2 after calcination.

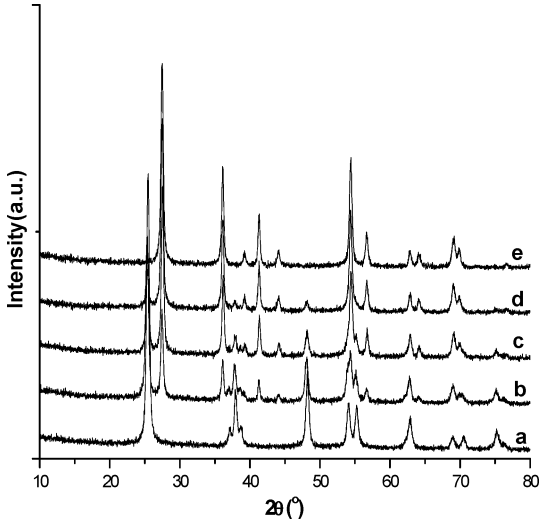

Figure 2. XRD patterns of MoO_3/TiO_2 samples with the molybdenum oxide loading amount of 0.20 mmol/100 m^2 TiO_2 and different rutile/TiO_2(R + A) ratios: (a) 0, (b) 0.25, (c) 0.50, (d) 0.75, and (e) 1.00, respectively.

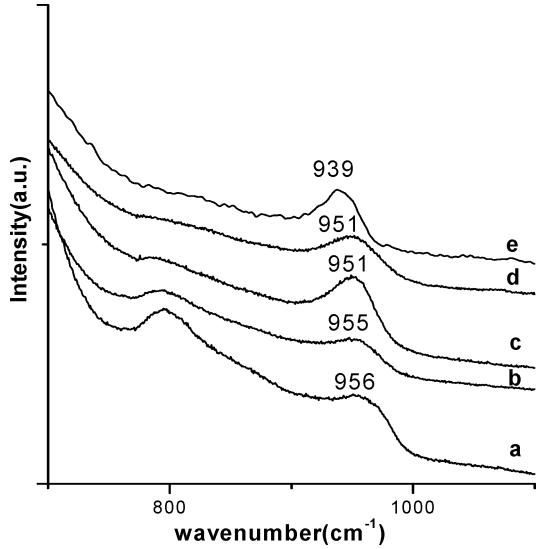

Figure 3. Raman spectra of MoO_3/TiO_2 samples with the molybdenum oxide loading amount of 0.20 mmol/100 m^2 TiO_2 and different rutile/TiO_2(R + A) ratios: (a) 0, (b) 0.25, (c) 0.50, (d) 0.75, and (e) 1.00, respectively.

Figure 2 shows the XRD patterns of MoO_3/TiO_2 samples with different rutile/TiO_2(R + A) ratios and the fixed molybdena loading amount of 0.20 mmol/100 m^2 TiO_2. It is clear that no diffraction peaks of crystalline MoO_3 can be detected, indicating that the molybdena species highly disperses on the surface of mixed TiO_2. Figure 3 shows the Raman spectra of these MoO_3/TiO_2 samples. The Raman bands of the terminal Mo═O stretching mode of the surface molybdena species in MoO_3/rutile and MoO_3/anatase are 939 and 956 cm^{-1}, respectively. When the BET surface area ratio of rutile/TiO_2(R + A) increases from 0.25 to 0.75, the Raman band of surface molybdena on mixed TiO_2 shifts from 955 to 951 cm^{-1}. As reported elsewhere,[24] for TiO_2 supported molybdena samples, the Raman band at >955 cm^{-1} is attributed to the symmetric stretching mode of the terminal Mo═O in the surface polymeric octahedral molybdena species, while the Raman band at ≤955 cm^{-1} is attributed to the terminal Mo═O in the surface isolated tetrahedral molybdena species. The Raman bands of surface molybdena in the mixed TiO_2 supported samples are all below 955 cm^{-1}. Therefore, it seems to propose that the surface molybdena species in mixed TiO_2 supported molybdena samples mainly exists in the isolated tetrahedral state. Furthermore, the results imply that, for the lower molybdena loading samples, molybdena would preferentially disperse on the surface of rutile in mixed TiO_2 and form the isolated tetrahedral molybdena species.

Figure 4A,B shows the TPR results of MoO_3/rutile and MoO_3/anatase samples, respectively. For a comparison, the TPR profiles of rutile and anatase are given in Figure 4A, spectrum a and 4B, spectrum a. It can be seen that the reduction peaks of rutile and anatase are higher than 550 °C. Therefore, the reduction peaks below 500 °C should be related to the reduction of the surface molybdena species. For the samples with the molybdena loading amount of 0.20 mmol/100 m^2 TiO_2, the reduction peaks of a surface molybdena species in MoO_3/rutile and MoO_3/anatase are at about 390 and 480 °C, respectively. It is well-acknowledged that the peaks should be attributed to the reduction of surface molybdena (i.e., $Mo^{6+} \rightarrow Mo^{4+}$).[12] The discrepancy of the reduction behaviors of surface molybdena in MoO_3/rutile and MoO_3/anatase should be due to the differences of the existing states of surface molybdena species. As reported elsewhere,[12] the reduction peak at about 390 °C is attributed to the reduction of surface molybdena species in a tetrahedral coordination state, while the peak at about 480 °C is attributed to the reduction of that in octahedral coordination state. Therefore, it could be concluded that the surface molybdena species on the surface of rutile and anatase exists as the tetrahedral and octahedral coordination state, respectively, which is basically consistent with the Raman results. With the molybdena loading amount increasing to 0.82 mmol/100 m^2 TiO_2 (i.e., the monolayer dispersion of molybdena on TiO_2),[25,26] the reduction peaks of the surface molybdena species in MoO_3/anatase and MoO_3/rutile both increase. It is noticeable that the baseline of Figure 4A, spectrum c rises from 440 to 570 °C, which might be due to the reduction of a polymeric molybdena species formed from the polymerization of the surface isolated tetrahedral molybdena species.[24]

Figure 5 shows the TPR results of MoO_3/TiO_2 samples with the fixed molybdena loading amount (0.20 mmol/100 m^2 TiO_2) and different rutile/TiO_2 ratios, from 0 to 1.0. It is clearly seen that, for increasing rutile content in the mixture support, the shapes of the profiles change greatly. Comparing spectra a and b, a new reduction peak centered at about 362 °C has appeared besides the peak at about 480 °C, and the H_2 consumption of spectrum b is evidently decreased more than that of spectrum a at the reduction temperature 480 °C. For spectra c−e, only one peak around 362 °C could be observed. Considering the fact that the varying composition of the TiO_2 mixture is from pure anatase to rutile, it seems reasonable to suggest that, for 0.20 mmol/100 m^2 TiO_2 samples, molybdena would preferentially disperse on the surface of rutile in mixed TiO_2.

To approach the relationship between the variation of the surface acidic and basic properties of the titania mixture and the molybdena modified titania mixture and the rutile/TiO_2(R + A) ratio and the molybdena loading amount, pyridine adsorption IR spectra have been recorded for this purpose. Figure 6A,B shows the FT−IR spectra at 1400−1800 cm^{-1} pyridine adsorption on MoO_3/rutile and MoO_3/anatase samples with different MoO_3 loading amounts, respectively. As reported elsewhere,[27] the bands at about 1445, 1573, and 1607 cm^{-1} should be attributed to the frequencies of pyridine adsorbed on the Lewis acid sites; the bands at about 1541 and 1634 cm^{-1} should be attributed to the frequencies of pyridine interacting

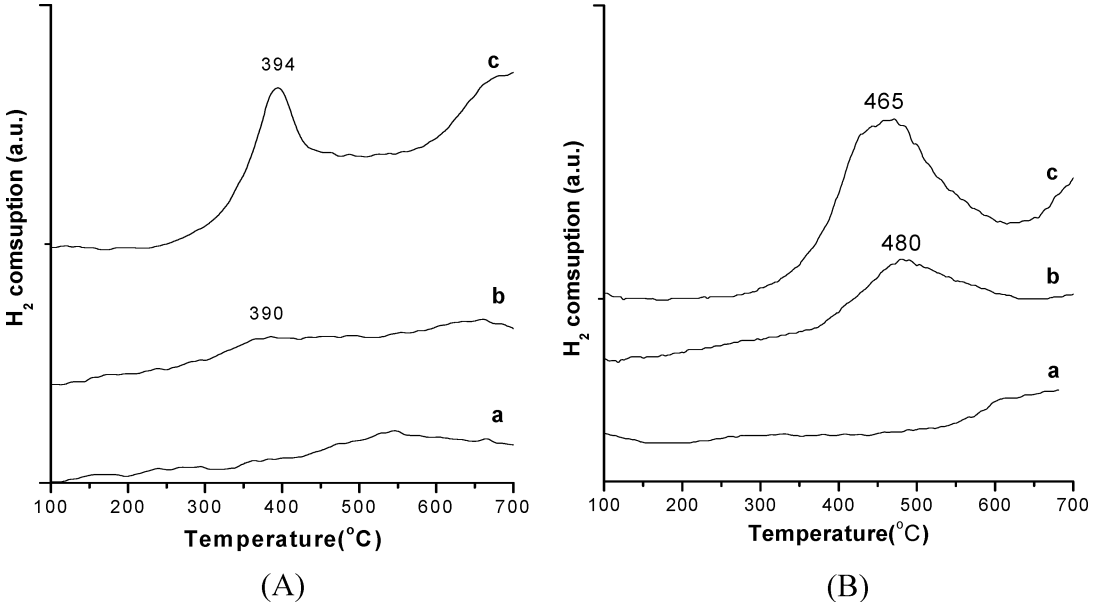

Figure 4. TPR profiles of MoO_3/rutile (A) and MoO_3/anatase (B) samples with different molybdenum oxide loading amounts: (a) 0, (b) 0.20, and (c) 0.82 mmol/100 m^2 TiO_2, respectively.

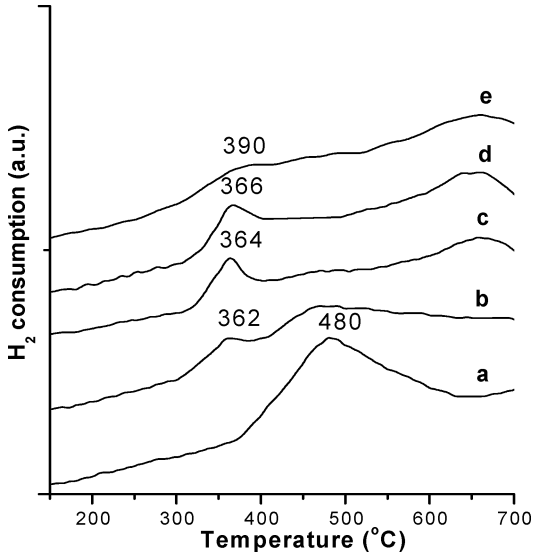

Figure 5. TPR profiles of MoO_3/TiO_2 samples with the molybdenum oxide loading amount of 0.20 mmol/100 m^2 TiO_2 and different rutile/TiO_2(R + A) ratios: (a) 0, (b) 0.25, (c) 0.50, (d) 0.75, and (e) 1.00, respectively.

with the Bronsted acid sites and the creation of PyH^+, while the bands at 1493 cm^{-1} should be attributed to the common contribution of pyridine adsorbed in Lewis acid sites and Bronsted acid sites. Shown as in Figure 6A, spectrum a, only the bands at about 1442, 1489, and 1605 cm^{-1} can be detected in the FT−IR spectra, indicating that the Lewis acid sites are the main acid ones on the surface of rutile. For the 02MoTi-100%r sample, the intensity of these three bands increases, and the bands corresponding to the Bronsted acid sites, at about 1541 and 1634 cm^{-1}, have not been detected. However, for the 082MoTi-100%r sample, a weak band at 1541 cm^{-1} appears in Figure 6A, spectrum c, indicating that a small amount of Bronsted acid sites have formed. Considering the results in the Raman and TPR methods that the isolated tetrahedral molybdena species in the 082Mo/Ti-100%r sample would polymerize and form the polymeric molybdena species, it seems reasonable to suggest that the formation of the Bronsted acid sites on the surface of rutile should be related to the creation of the polymeric molybdena species. For the 02MoTi-0%r and 082Mo-Ti-0%r samples presented in Figure 6B, spectra b and c, the band at 1541 cm^{-1} related to PyH^+ (Bronsted acid sites) can also be found besides the 1445, 1493, and 1607 bands corresponding to the Lewis acid sites, which implies that the molybdena species exists in the polymeric molybdena species in these two samples. In addition, Primet et al. have investigated the acidic and basic properties of rutile and anatase, and their results suggested that some OH groups of anatase show a protonic character toward $(CH_3)_3N$ (i.e., a strong basic probe molecule) but not NH_3 and C_5H_5N, and no protonic character has been detected for rutile.[28] Therefore, it can be concluded that the formation of the Bronsted acid sites should be related to the creation of the surface polymeric molybdena species.

Figure 7 shows the FT−IR spectra in the 1400−1800 cm^{-1} pyridine adsorption on the 02MoTi-50%r, 02MoTi-0%r, and 02MoTi-100%r samples. For these spectra, the bands at 1445, 1492, and 1607 cm^{-1}, relating to the Lewis acid sites, could be clearly detected. Comparing spectra a and b, no trace of the band at 1541 cm^{-1}, relating to the Bronsted acid sites, could be detected in 02MoTi-50%r sample, which means that the dispersed molybdena mainly exist on the surface of rutile because of the dispersed molybdena on the surface of anatase creating the Bronsted acid sites. The results also suggest that molybdenum oxide would preferentially disperse on the surface of rutile in mixed TiO_2.

It is well-established that the surface of metal oxides is covered by the hydroxyl group via the dissociation of the adsorbed H_2O in air and that the hydroxyl group plays an important role in the adsorption processes occurring at the oxide surface.[29,30] Figure 8 shows the schematic diagram of the dissociation of the adsorbed H_2O on the surface of TiO_2. As depicted in Figure 8, the dissociation of a H_2O molecule would form two types of hydroxyl groups. The OH group associated with Ti^{4+} ions is designated as OH_b, while the H^+ ion associated with the surface crystalline O^{2-} anions is designated as OH_a. Obviously, the OH_b group would have stronger basicity than the OH_a group. Accordingly, the discrepant surface physicochemical properties of rutile and anatase, especially for the acidic and basic properties of surface OH groups resulting from their

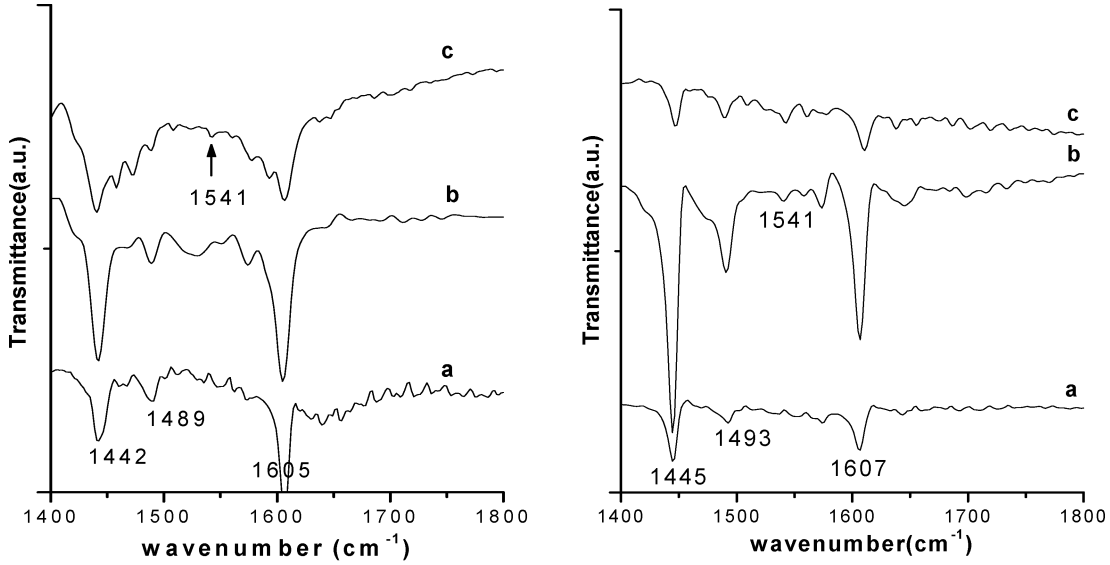

Figure 6. FT−IR spectra in 1400−1800 cm^{-1} pyridine adsorption on MoO_3/rutile (A) and MoO_3/anatase (B) samples with different MoO_3 loading amounts: (a) 0, (b) 0.20, and (c) 0.82 mmol/100 m^2 TiO_2, respectively.

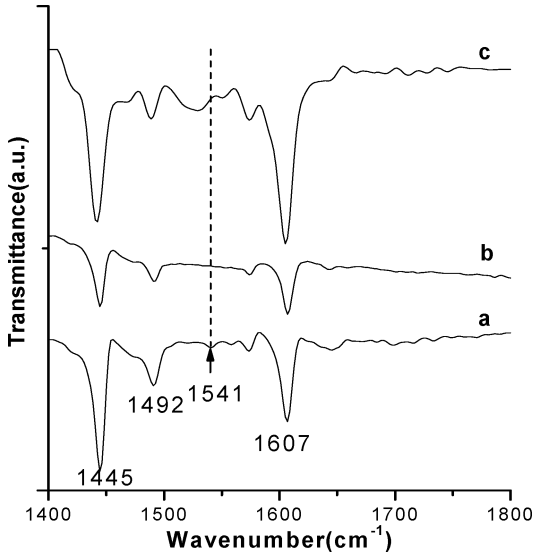

Figure 7. FT−IR spectra in 1400−1800 cm^{-1} pyridine adsorption on $02MoO_3$/anatase (a), 02MoTi-50%r (b), and $02MoO_3$/rutile (c), respectively.

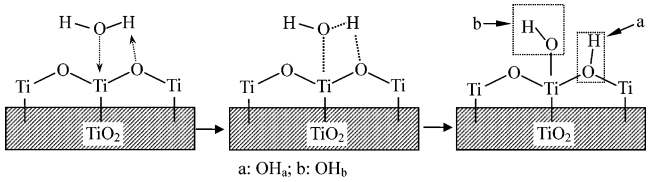

Figure 8. Schematic diagram of the dissociation of the adsorbed H_2O on the surface of TiO_2.

different crystalline phases and surface structures, would influence the interaction between molybdena oxide and oxide supports.

Primet et al. have investigated the IR spectra of the OH groups of anatase and rutile. The results suggest that there are two and three types of OH groups on anatase and rutile, respectively, which should be related to the positions of these groups in the crystalline lattice.[31] They suggest that the cleavage plane of titania determines the types of these OH groups.[31] As reported elsewhere,[31,32] the (110) plane and the (001) plane are the preferentially exposed plane of rutile and anatase, respectively. In rutile and anatase, each Ti^{4+} ion is surrounded by six O^{2-} anions, each O^{2-} ion has three Ti^{4+} neighbors, and the net charge of O^{2-} ion is +2/3 gained from each neighboring Ti^{4+} ion.[29] Therefore, according to the interaction with Ti^{4+} ions or the net charge of the OH group, the OH group would show different acidic and basic properties. Generally speaking, the more negative the net charge of the OH group is, the more basic the OH group is. For rutile, surface OH groups could be divided to three types, designated as $R-OH_b$, $R-OH_{b'}$, and $R-OH_a$, respectively. The net charges of $R-OH_b$, $R-OH_{b'}$, and $R-OH_a$ are −1/3, +1/3, and +1, respectively.[25,29] So, the acidity of these OH groups would increase in the order $R-OH_b < R-OH_{b'} < R-OH_a$. For anatase, surface OH groups could be ascribed to two types (i.e., A-OH_a and A-OH_b), the net charges of which are −1/3 and +1/3. As suggested by Wachs et al.,[30] the dispersion of molybdena on TiO_2 could be regarded as the dehydration of surface OH groups between molybdena and TiO_2. Considering that molybdena is an acidic oxide and that the OH groups on the molybdena surface would show the acidic property,[32] it could be supposed that the OH group of molybdena would preferentially interact with the OH group that has the stronger basicity on the TiO_2 surface. As shown in Primet's report,[31] the frequencies of the OH stretching vibrations of $R-OH_b$ and $A-OH_b$ are 3685 and 3715 cm^{-1}, respectively, and they suggest that the hydroxylic hydrogen atom about $A-OH_b$ is more protonic than that about $R-OH_b$ (i.e., the basicity of $R-OH_b$ is relatively stronger than that of $A-OH_b$). Consequently, it seems to be predicted that, for the lower molybdena loadings, the OH groups of molybdena would preferentially interact with $R-OH_b$ to dehydrate during calcinations and form the dispersed surface molybdena species and that this deduction has been certified by the Raman, FT−IR, and TPR results.

On the basis of the previous discussion, it seems reasonable to tentatively approach the surface states of the dispersed molybdena on anatase and rutile by considering the preferential interaction between the OH groups of molybdena and $A-OH_b$ and $R-OH_b$, respectively. For MoO_3/rutile samples with a low

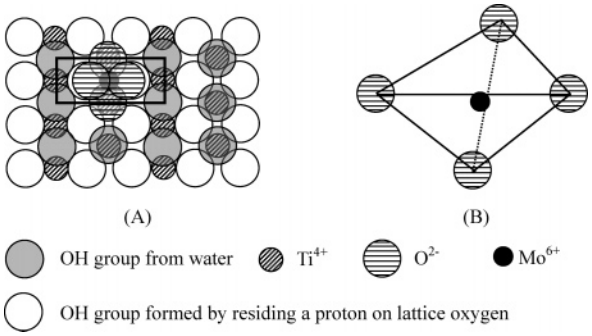

Figure 9. Schematic diagram of a molybdenum oxide molecule on the (110) plane of rutile (A) and the coordination structure of a surface Mo^{6+} ion (B).

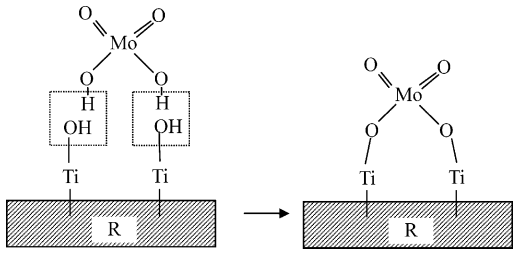

Figure 10. Schematic diagram of the dehydration of surface OH groups between a molybdenum oxide molecule and rutile.

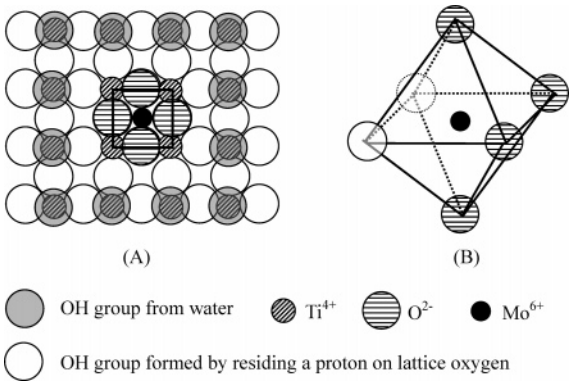

Figure 11. Schematic diagram of a molybdenum oxide molecule on the (001) plane of anatase (A) and the coordination structure of a surface Mo^{6+} ion (B).

molybdena loading amount, as shown in Figure 9, the OH groups of molybdena could interact with two $R-OH_b$ groups on the rutile surface and form the isolated tetrahedral species during the calcination procedure, and the dehydration process of the groups of a molybdena molecule could be depicted in Figure 10. The OH groups of molybdena would lose the proton, while the $R-OH_b$ groups on the rutile surface would lose the OH^- group. When the molybdena loading amount increases to a certain content, the $R-OH_b$ groups have been consumed completely, and the molybdena species would interact with the $R-OH_b$, groups and polymerize on the rutile surface. For MoO_3/anatase samples, with the same consideration mentioned previously, molybdena could interact with the groups on the anatase surface and form the dispersed molybdena species. As shown in Figure 11, a formed surface molybdena species would have an octahedral coordination environment.

Conclusions

(1) For the $MoO_3/TiO_2(R + A)$ samples with lower molybdena loading, LRS and pyridine adsorption of FT−IR and TPR results suggest that molybdena would preferentially disperse on the rutile surface in mixed TiO_2.

(2) On the basis of the consideration of the preferentially exposed plane of rutile and anatase, the surface environments of the dispersed molybdena species have been suggested as (a) for MoO_3/rutile with low molybdena loading (e.g., 0.20 mmol/100 m^2 rutile), the dispersed molybdena species on the rutile surface is in an isolated tetrahedral coordination environment, and when the molybdena loading was increased, the isolated tetrahedral molybdena species would polymerize and (b) for the MoO_3/anatase sample, the dispersed molybdena species exist on the anatase surface as octahedral coordination environment.

(3) The different states of the dispersed molybdena species should result from the different dehydration orders of OH groups of the molybdena and surface OH groups of rutile and anatase. The basicity of $R-OH_b$ is relatively stronger than that of $A-OH_b$, and consequently, the OH group of molybdena would preferentially dehydrate with the $R-OH_b$ group, especially for the lower molybdena loading, to form the dispersed molybdena species on the surface of rutile during the calcination.

Acknowledgment. The financial support of the Specialized Research Fund for the Doctoral Program of Higher Education (Grant 20030284002), the pre-research foundation for the important program of Nanjing University, and the National Basic Research Program of China (Grant 2003CB615804) are gratefully acknowledged.

References and Notes

(1) Massooth, F. E. *Adv. Catal.* **1978**, *27*, 265.
(2) Knozinger, H. In *Proceedings of the 9th International Congress on Catalysis, Calgary, 1988*; Phillips, M., Ternan, M., Eds.; The Chemical Institute of Canada: Ottawa, 1989; Vol. 5, p 20.
(3) Reddy, B. M.; Chary, K. V. R.; Subrahmanyam, V. S.; Nag, N. K. *J. Chem. Soc., Faraday Trans. 1* **1985**, *81*, 1655.
(4) Ng, K. Y. S.; Gulari, E. *J. Catal.* **1985**, *95*, 33.
(5) Liu, Y. C.; Griffin, G. L.; Chan, S. S., Wachs, I. E. *J. Catal.* **1985**, *94*, 108.
(6) Masuoka, Y.; Niwa, M.; Murakami, Y. *J. Phys. Chem.* **1990**, *94*, 1477.
(7) Zhang, W.; Desikan, A.; Oyama, S. T. *J. Phys. Chem.* **1995**, *99*, 14468.
(8) Nag, N. K. *J. Phys. Chem.* **1987**, *91*, 2324.
(9) Quincy, B. R.; Houalla, M.; Proctor, A.; Hercules, D. M. *J. Phys. Chem.* **1990**, *94*, 1520. Reddy, B. M.; Chowdhury, B. *J. Catal.* **1998**, *179*, 413.
(10) Desikan, A. N.; Huang, L.; Oyama, S. T. *J. Phys. Chem.* **1991**, *95*, 10050.
(11) Desikan, A. N.; Huang, L.; Oyama, S. T. *J. Chem. Soc., Faraday Trans.* **1992**, *88*, 3357.
(12) Bond, G. C.; Tahir, S. F. *Appl. Catal.* **1993**, *105*, 281.
(13) Arco, D. M.; Holgado, J. M.; Martin, C.; Rives, V. *J. Catal.* **1986**, *99*, 19.
(14) Machej, T.; Haber, J.; Turek, M. A.; Wachs, I. E. *Appl. Catal.* **1991**, *70*, 115.
(15) Kim, D. S.; Kurusu, Y.; Wachs, I. E.; Hardcastle, F. D.; Segawa, K. *J. Catal.* **1989**, *120*, 325.
(16) Xu, B. L.; Fan, Y. N.; Liu, L.; Lin, M.; Chen, Y. *Sci. China, Ser. B* **2002**, *45*, 407.
(17) Matsuda, S.; Kato, A. *Appl. Catal.* **1983**, *8*, 149.
(18) Reiche, M. A.; Ortelli, E.; Baiker, A. *Appl. Catal. B* **1999**, *23*, 187.
(19) Dunn, J. P.; Koppula, P. R.; Stenger, H. G.; Wachs, I. E. *Appl. Catal. B* **1998**, *19*, 103.
(20) Ng, K. Y. S.; Gulari, E. *J. Catal.* **1983**, *92*, 340.
(21) Kim, D. S.; Segawa, K.; Soeya, T.; Wachs, I. E. *J. Catal.* **1992**, *136*, 539.
(22) Kim, D. S.; Wachs, I. E.; Segawa, K. *J. Catal.* **1994**, *146*, 268.
(23) Ohno, T.; Tokieda, K.; Higashida, S.; Matsumura, M. *Appl. Catal. A* **2003**, *244*, 383.
(24) Ng, K. Y. S.; Gulari, E. *J. Catal.* **1985**, *92*, 340.
(25) Chen, Y.; Zhang, L. F. *Catal. Lett.* **1992**, *12*, 51.
(26) Liu, Y. J.; Xie, Y. C.; Ming, J.; Liu, J.; Tang, Y. Q. *J. Catal. (China)* **1982**, *3*, 262.

(27) Bezrodna, T.; Puchkovska, G.; Shimanovska, V.; Chashechnikova, I.; Khalyavka, T.; Baran, J. *Appl. Surf. Sci.* **2003**, *214*, 222.
(28) Primet, M.; Pichat, P.; Mathieu, M. V. *J. Phys. Chem*. **1971**, *75*, 1221.
(29) Boehm, H. P. *Adv. Catal.* **1966**, *16*, 179.
(30) Wachs, I. E.; Saleh, R. Y.; Chan, S. S.; Chersich, C. C. *Appl. Catal.* **1985**, *15*, 339.
(31) Primet, M.; Pichat, P.; Mathieu, M. V. *J. Phys. Chem*. **1971**, *75*, 1216.
(32) Knozinger, H. *Adv. Catal*. **1976**, *25*, 184.